

## Pressure-induced hard-to-soft transition of a single carbon nanotube

D. Y. Sun,<sup>1</sup> D. J. Shu,<sup>1</sup> M. Ji,<sup>2</sup> Feng Liu,<sup>3</sup> M. Wang,<sup>4</sup> and X. G. Gong<sup>2,1,\*</sup>

<sup>1</sup>*Institute of Solid State Physics, Academia Sinica, 230031-Hefei, China*

<sup>2</sup>*National Laboratory of Surface Science and Department of Physics, Fudan University, Shanghai 200433, China*

<sup>3</sup>*University of Utah, Salt Lake City, Utah 84112, USA*

<sup>4</sup>*National Laboratory of Solid State Microstructures, Nanjing University, Nanjing 210093, China*

(Received 30 October 2003; revised manuscript received 23 August 2004; published 22 October 2004)

We demonstrate a hydrostatic pressure-induced hard-to-soft transition of an isolated single wall carbon nanotube, using classical and *ab initio* constant-pressure molecular-dynamics simulations and continuum elastic theory analysis. At low pressure, the carbon tube is hard. Above a critical pressure, the tube becomes much softer with a decrease of bulk modulus by two orders of magnitude. The hard-to-soft transition is caused by a pressure-induced shape transition of the tube cross section from circular to elliptical.

DOI: 10.1103/PhysRevB.70.165417

PACS number(s): 61.48.+c, 62.20.-x, 62.50.+p

Carbon nanotubes (NTs) exhibit a wealth of fascinating structural, mechanical, and electronic properties. As an ideal one-dimensional structure, their properties are highly anisotropic. For example, mechanically the NTs are extraordinarily hard in the axial direction but soft in the radial direction; the compressibility anisotropy in the two directions exceeds orders of magnitude. As the NTs are virtually incompressible in the axial direction, much attention has been paid to their structural and mechanical behavior in the radial direction.<sup>1-8</sup> The radial deformation (i.e., the change of cross-section shape) of single-walled carbon nanotubes (SWNTs) in turn influences their mechanical<sup>1-5</sup> and electronic properties.<sup>7-9</sup>

The hardness, as one of the most important parameters characterizing the mechanical properties of SWNTs, has been intensively studied.<sup>10-12</sup> However, so far, most studies have focused only on the ground-state hardness of SWNTs at ambient conditions. In this Paper, we investigate the mechanical properties, especially the hardness, of a single SWNT under hydrostatic pressure, using constant-pressure molecular-dynamics (MD) simulations and linear elastic analysis. We discover a pressure-induced hard-to-soft transition at which the radial modulus of the SWNT decreases by as much as two orders of magnitude. We show that this mechanical (hardness) transition is caused by a pressure-induced structural (shape) transition of SWNT characterized by a transformation of its cross section from a circular to elliptical shape. The critical transition pressure decreases with increasing tube radius.

We use a constant-pressure MD method especially suited for simulating finite system.<sup>13</sup> Specifically for a single NT, the volume is calculated by numerically evaluating the tube cross-section area enclosed by the atoms from atomic positions.<sup>13</sup> We use the periodic boundary condition in the axial direction and free boundary condition in the radial directions. The interaction between carbon atoms is described by a parametrized many-body potential,<sup>14</sup> which has been widely used to study mechanical properties of carbon NT.<sup>1,15,16</sup> To confirm the results of the classical molecular dynamics method, we have simulated single (6,6) tube by *ab initio* molecular dynamics method.

We have simulated SWNTs of different radii ranging from (5,5) to (20,20) under hydrostatic pressure. All the NTs un-

dergo a pressure-induced hard-to-soft phase transition. The *hard* phase at low pressure exhibits a typical bulk modulus of 100 GPa, while the *soft* phase at high pressure exhibits a bulk modulus of only  $\sim 1$  GPa. Figure 1 shows the pressure and the total energy as a function of reduced volume for a (10,10) nanotube at 300 K, where the energy at zero pressure is set to zero. Clearly, a transition at  $\sim 1.0$  GPa is observed. Below the transition, the *hard* phase has a radial compressibility of  $0.01 \text{ GPa}^{-1}$ . Above the transition, the *soft* phase has a radial compressibility about two orders of magnitude larger.

The hard-to-soft transition is caused by a pressure-induced circular-to-elliptical shape transition in the cross section of SWNT. Figure 2 shows the evolution of the cross-section shape, the bond length, and the bond angle with increasing pressure for a (10,10) nanotube. We use the length of the two principal axes, long axis  $a$  and short axis  $b$ , to

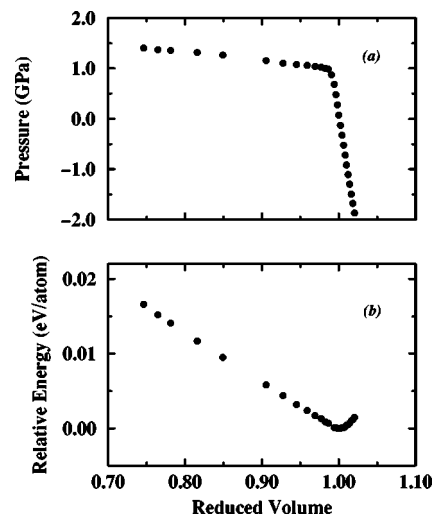


FIG. 1. The energy and pressure as a function of the reduced volume for (10,10) nanotube at 300 K. The energies are relative to the minimum energy, and the volume is normalized by the equilibrium volume without the external pressure. At about 1.0 GPa, the *hard* phase with bulk modulus of about 100 GPa transforms into the *soft* phase with bulk modulus of just a few GPa.

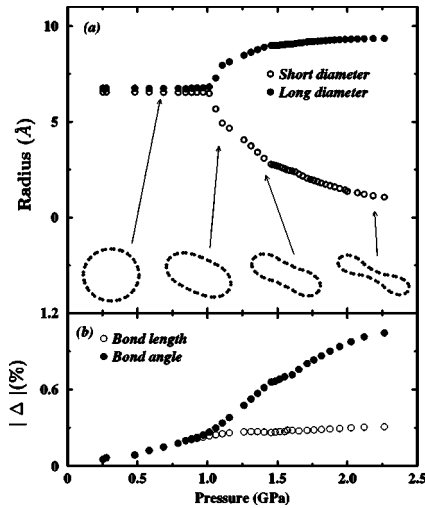


FIG. 2. (a) The length of the long and short axes, as a function of pressure for (10,10) nanotube. The shape of the cross section at some selected pressures is plotted at the bottom of the figure. (b) The absolute relative change of bond length and bond angle as a function of pressure for (10,10) nanotube, the data is obtained by quenching the system from 300 to 0 K at constant pressure.

characterize an elliptical shape. Below the transition pressure,  $\sim 1.0$  GPa,  $a$  remains almost equal to  $b$ , defining a circular shape. Above  $\sim 1.0$  GPa,  $a$  becomes larger than  $b$ , defining an elliptical shape. The aspect ratio ( $a/b$ ) of the elliptical shape increases continuously with increasing pressure. Eventually, as the long axis continues to increase and the short axis continues to decrease, the elliptical shape undergoes another transition to a dumbbell shape, as shown in Fig. 2(a). Under even higher pressure, the dumbbell tube can become so flat that the spacing between the opposite side walls approaches the layer spacing in the graphite ( $\sim 3.35$  Å). Consequently, there will be an additional van der Waals interaction between the side walls that can lead to the collapse of the tube.<sup>17</sup> Such an effect is more pronounced for tubes with larger radii. Here, however, we focus on the hardness transition in the pressure regime above the collapsing and all the NTs we studied are well below the critical radius for collapsing without pressure.<sup>17</sup>

Figure 2(b) shows that the percentage change in bond length and bond angle increases simultaneously with increasing pressure below the transition, indicating a uniform shrinking of the circular shape under pressure. Above the transition, the bond length remains unchanged but the change of bond angle increases sharply with increasing pressure. The trend of change in bond length and bond angle provides a good explanation of the hard-to-soft transition. It costs much more energy to change bond length than to change bond angle. Below the transition, the structural response to the external pressure is largely taken by the changing bond length of a circular shape, giving rise to a hard phase; while above the transition, the structural response to the external pressure is largely taken by the changing bond angle of an elliptical shape, giving rise to a soft phase.

The critical transition pressure depends strongly on the tube radius. Figure 3 shows the simulated transition pres-

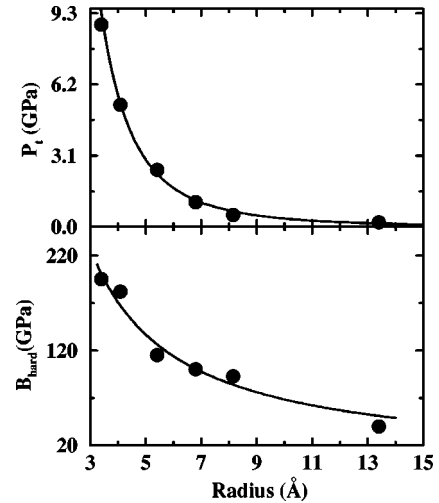


FIG. 3. The transition pressure (upper panel) and the elastic modulus (lower panel) as a function of tube radius at 300 K. The solid line is a least-squares fit to the data using Eq. (4) (upper panel) and Eq. (6) (lower panel). The simulated data follows nicely with the predicted behavior.

ures (solid dots) at 300 K to be 8.8, 5.3, 2.2, 1.0, 0.5, and 0.2 GPa for the (5,5), (6,6), (8,8), (10,10), (12,12), and (20,20) nanotubes, respectively. The smaller the radius, the higher the transition pressure.<sup>18</sup>

To confirm the pressure-induced shape and hardness transition of SWNTs which is discovered by our molecular-dynamics simulations using classical interatomic potential, we have also simulated the behavior of a (6,6) carbon nanotube under hydrostatic pressure by *ab initio* molecular dynamics, using the pseudopotential plane-wave method ( $E_{\text{cut}} = 286$  eV) and the generalized gradient approximation energy functional. The similar calculation methods have been successfully used to study the graphite systems.<sup>19–21</sup> To simulate a “single” tube, a supercell with a large dimension ( $16$  Å  $\times$   $16$  Å) in the  $x$ - $y$  plane (i.e., the plane of the tube cross section) is used to exclude the interaction between the tube and its periodic images. Forty-eight atoms are included in the simulation cell, two special  $k$  points are used in the Brillouin zone sampling. Figure 4 shows the results of simulated volume, energy, and shape (lengths of long and short axes of ellipse) as a function of applied pressure. They are very similar to the results of the (10,10) tube simulated by classical potential, as shown in Figs. 1 and 2. Clearly, *ab initio* simulations confirm qualitatively the pressure-induced transition found by the classical potential. Quantitatively, however, the *ab initio* potential predicts a transition pressure of  $\sim 10$  GPa, which is about two times the value  $\sim 5.3$ , predicted by classical potential. This indicates the classical potential is somewhat too soft, which is known for the Tersoff-type potential. We also note that the classical potential does not include the van der Waals interaction between the tube walls. However, we found that inclusion of such interaction in the classical potential does not change the results noticeably. This is not surprising because the van der Waals interaction becomes only significant when the distance between the tube walls is small ( $< 3.4$  Å), while the actual distance at

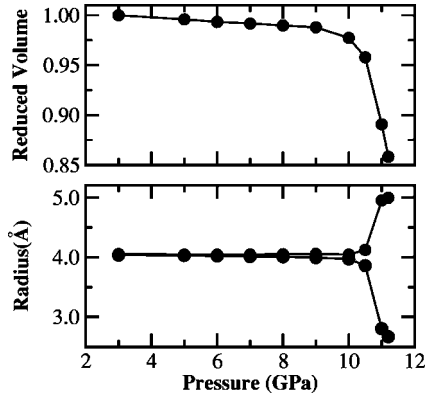


FIG. 4. The energy and pressure as a function of the reduced volume for (6,6) nanotube at 300 K, obtained by *ab initio* molecular dynamics. The energies are relative to the minimum energy, and the volume is normalized by the equilibrium volume without the external pressure. The hard to soft transition can be observed at about 10.5 GP.

the transition pressure for all the tubes is much larger and remains so even for deformed tubes in most cases. Although the classical potential predicts a lower value of individual transition pressure, it correctly predicts the qualitative behavior, including the dependence of transition pressure on tube radius, in good agreement with continuum theory, as we discuss below.

Next, we provide a general analysis and understanding of the above simulation results, especially the hard-to-soft transition, based on continuum linear elastic theory. Consider an original circular nanotube of radius  $R_0$  being transformed into an elliptical shape, the energy per length of tube, in reference to the energy of original tube, can be expressed as<sup>22,23</sup>

$$E = \frac{D}{2} \oint \frac{1}{\rho^2} dl + \frac{C}{2} \oint \left( \frac{\oint dl - L_0}{L_0} \right)^2 dl + PA, \quad (1)$$

where  $D = Yh^3/12(1-\nu^2)$  and  $C = Yh/(1-\nu^2)$  are constants related to Young's modulus ( $Y$ ), Poisson ratio ( $\nu$ ), and the tube thickness ( $h$ ).  $\rho$  is the radius of local curvature.  $L_0 = 2\pi R_0$  is the perimeter of the original tube cross section.  $A$  is the area of tube cross section. Here the first term represents the bending strain energy and the second term represents the compression strain energy.

For an elliptical shape with long axis  $a$  and short axis  $b$  and introducing  $R = \sqrt{ab}$ ,  $\omega = b/a$ , and  $\epsilon = R(f_2(\omega) - R_0)/R_0$  the strain of the bond length. The integration of Eq. (1) gives

$$E = D\pi \frac{f_1(\omega)f_2(\omega)}{R_0(1+\epsilon)} + C\pi\epsilon^2 R_0(1+\epsilon) + P\pi R_0^2 \frac{(1+\epsilon)^2}{f_2^2(\omega)}, \quad (2)$$

with

$$f_{1,2}(\omega) = \frac{1}{2\pi} \oint (\omega \cos^2 t + \omega^{-1} \sin^2 t)^{\alpha_{1,2}} dt, \quad (3)$$

$$\alpha_1 = -5/2 \text{ and } \alpha_2 = 1/2.$$

The optimal shape under a given pressure is then determined by the energy minimization with respect to variables  $\epsilon$  and  $\omega$ . Because both functions  $f_1(\omega)$  and  $f_2(\omega)$  have a minimum at  $\omega = 1$ , it is easy to see that the first term in Eq. (2) has a minimum at  $\omega = 1$ , favoring an isotropic circular shape while the third term has a maximum at  $\omega = 1$ , favoring an anisotropic elliptical shape. Consequently, at low pressure when the first term dominates, the tube adopts a circular shape with an energy minimum at  $\omega = 1$ , and the in-plane strain  $\epsilon$  changes with pressure  $P$  as  $\epsilon(P) = D/2CR_0^2 - PR_0/C$ . At high pressure when the third term becomes dominant, the tube adopts an elliptical shape with an energy minimum at  $\omega \neq 1$ , with both  $\epsilon$  and  $\omega$  changing with the pressure as

$$P(\epsilon, \omega) = \frac{Df_2^4(\omega)}{2R_0^3(1+\epsilon)^3} \left( \frac{f_1'(\omega)}{f_2'(\omega)} + \frac{f_1(\omega)}{f_2(\omega)} \right), \quad (4)$$

$$\epsilon(\omega) = -\frac{Df_2^2(\omega)f_1'(\omega)}{2CR_0^2f_2'(\omega)}, \quad \frac{d\omega}{d\epsilon} = \frac{CR_0^2}{10Df_2'}. \quad (5)$$

The above equations clearly indicate a phase transformation at certain critical pressure  $P_t$ . Above the critical pressure, the cross section changes from circular ( $\omega = 1$ ) to elliptical ( $\omega < 1$ ), associated with abrupt changes of strain, cross-sectional area. Note that the strain  $\epsilon$  is very small even under large pressure, whereas the deformation of the cross section can be very large. The reason for such a behavior is, for single-walled nanotubes,  $D/CR^2 = h/R \ll 1$ .

It is interesting to note that such a pressure-induced nanotube shape instability resembles a somewhat physical phenomenon occurring in epitaxial growth where stress (strain) induces a shape instability in a two-dimensional island and drives it to transform from an isotropic to an anisotropic shape.<sup>24</sup>

The critical transition pressure is defined by the conditions  $d^2E/d\omega^2|_{\omega=1} = 0$  and  $dE/d\epsilon|_{\omega=1} = 0$ , which give rise to

$$P_t = \frac{3D}{R_0^3(1+\epsilon_c)^3} \approx \frac{3D}{R_0^3}, \quad (6)$$

$$\epsilon_c = -\frac{5D}{2CR}. \quad (7)$$

This analytical dependence of  $P_t$  on  $R_0$  is in very good agreement with the MD simulations, as shown in Fig. 3. The elastic constant  $D$  (also  $C$ ) may depend weakly on tube radius. Nevertheless, treating it independent of tube radius, a least-squares fit to the simulation data yields a value of  $D = 0.76$  eV, in good agreement with previous results.<sup>1,10,15</sup> The tube first shrinks very slightly to  $\epsilon_c$  before the transition taking place; the larger the tube, the sooner the transition occurs.

The pressure-induced shape transition in turn induces a

hardness transition. The bulk modulus of the *hard* phase can easily be calculated as

$$B_h = \frac{C}{2R_0}. \quad (8)$$

The radial modulus of the *soft* phase can also be calculated, after some algebra and numerical differentiation of  $f_1(\omega)$  and  $f_2(\omega)$ , as

$$B_s \approx \frac{19D}{2R_0^3}. \quad (9)$$

Below the transition, the tube remains circular and the effect of pressure is to reduce the tube radius (bond length), and the hard-phase modulus [Eq. (6)] is related only to constant  $C$ , representing the compression energy. Above the transition, the effect of pressure is to change the tube shape (bond angle) and the soft-phase modulus [Eq. (7)] is related only to constant  $D$ , representing the bending energy. The ratio of bulk modulus in the soft and hard phases is

$$\frac{B_s}{B_h} = \frac{19}{12} \left( \frac{h}{R_0} \right)^2. \quad (10)$$

In general, the tube thickness is much smaller than the tube radius. Consequently, the radial modulus of the soft phase is much smaller than that of the hard phase. For example, using a tube thickness of  $0.66 \text{ \AA}$ ,<sup>10</sup> about one tenth of the (10,10) tube radius, the ratio of the soft- to hard-phase modulus is estimated to be  $\sim 0.015$  for the (10,10) tube, in very good agreement with the MD simulation results. As the tube thickness is independent of the tube radius, the ratio of modulus decreases with increasing radius, i.e., the larger the tube, the more prominent is the hardness transition.

Recently, several experiments have indicated a structural transition in a bundle of SWNTs under hydrostatic pressure at the range of 1.5–1.7 GPa,<sup>2–5</sup> a circular-to-elliptical shape transition is suggested<sup>2,3</sup> and shown by MD simulations.<sup>4</sup> The transition is also shown to be reversible, indicating the structural deformation remains in the linear elastic regime. However, the physical origin and the nature of this pressure-induced transition remains unclear. It is interesting to speculate that our findings here in a single SWNT might shed some light to the understanding of the pressure-induced transition in a bundle of SWNTs. For a bundle of tubes, the intertube van der Waals interaction is an important additional factor in determining the tube properties. For example, the intertube interaction transforms the tube from a circle to a

polygon at large tube radius.<sup>1,6</sup> The physical origin of the polygonization transition is to increase the intertube interaction energy to overcome the elastic deformation energy of individual tube. Similarly, one might expect that the pressure-induced circular-to-elliptical transition in a bundle of SWNTs at high pressure is also caused by the intertube interaction. However, based on the behavior of single SWNT we discovered here, we suggest that the circular-to-elliptical transition in a bundle of SWNTs at high pressure is mainly driven by the pressure-induced intrinsic shape instability in each individual tube to minimize the elastic energy, while the intertube interaction plays a lesser role.

It is noteworthy that in Eq. (1) the area of the of the cross section of the nanotube is defined as  $\pi R^2$ . If we define the cross-section area as  $2\pi R h$ , however there is no transformation on both cross-sectional shape and the radial modulus. In the latter case, we actually assume that the pressure inside and outside of the nanotube is identical. This suggests that if the hydrostatic pressure can somehow enter the carbon nanotube, for example, via very large defects on the tube surface or via the opening ends of the nanotube, the cross section of the nanotube will remain circular and the tubes will keep the original radial modulus upon pressure. The fact that cross-sectional transformation of the nanotubes has indeed been observed<sup>2,25</sup> implies that in their case the external pressure or force did not damage the nanotubes.

In conclusion, using both MD simulations and continuum analysis, we demonstrate a pressure-induced hard-to-soft transitions in a single SWNT upon which the modulus of the NT decreases by as much as two orders of magnitude. We show that this mechanical transition is caused by a pressure-induced structural transition that not only transforms the cross section of the tube from circular to elliptical, but also changes the physical mechanism for mechanical response to external pressure from changing bond length to changing bond angle. Both simulations and analysis show that the critical pressure decreases with increasing tube radius in a third power law and the ratio of modulus in the hard and soft phases scales with the square of the tube radius. Furthermore, our findings in single SWNTs may provide some hints to the understanding of the pressure-induced transition in a bundle of SWNTs.

The authors thank Dr. X. M. Duan for technical assistance. This work is supported by the National Natural Science Foundation of China, the special funds for major state basic research and CAS projects. F.L. thanks the support from US DOE, Grant No. DE-FG03-01ER45875 and from NSFC for his visit to China.

\*Corresponding author; electronic mail: xggong@fudan.edu.cn

<sup>1</sup>J. Tersoff and R. S. Ruoff, Phys. Rev. Lett. **73**, 676 (1994).

<sup>2</sup>S. A. Chesnokov, V. A. Nalimova, A. G. Rinzler, R. E. Smalley, and J. E. Fischer, Phys. Rev. Lett. **82**, 343 (1999).

<sup>3</sup>U. D. Venkateswaran, A. M. Rao, E. Richter, M. Menon, A. Rinzler, R. E. Smalley, and P. C. Eklund, Phys. Rev. B **59**, 10 928

(1999).

<sup>4</sup>M. Peters, L. E. McNeil, J. P. Lu, and D. Kahn, Phys. Rev. B **61**, 5939 (2000).

<sup>5</sup>Jie Tang, Lu-Chang Qin, T. Sasaki, M. Yudasaka, A. Matsushita, and S. Iijima, Phys. Rev. Lett. **85**, 1887 (2000).

<sup>6</sup>M. J. Lopez, A. Rubio, J. A. Alonso, L.-C. Qin, and S. Iijima,

- Phys. Rev. Lett. **86**, 3056 (2001).
- <sup>7</sup>J.-C. Charlier, Ph. Lambin, and T. W. Ebbesen, Phys. Rev. B **54**, R8377 (1996).
- <sup>8</sup>C.-J. Park, Y-H. Kim, and K. J. Chang, Phys. Rev. B **60**, 10 656 (1999).
- <sup>9</sup>M. S. C. Mazzoni and H. Chacham, Appl. Phys. Lett. **76**, 1561 (2000).
- <sup>10</sup>B. I. Yakobson, C. J. Brabec, and J. Bernholc, Phys. Rev. Lett. **76**, 2511 (1996).
- <sup>11</sup>J. P. Lu, Phys. Rev. Lett. **79**, 1297 (1997).
- <sup>12</sup>E. W. Wong, P. E. Sheehan, and C. M. Lieber, Science **277**, 1971 (1997).
- <sup>13</sup>D. Y. Sun and X. G. Gong, J. Phys.: Condens. Matter **14**, L487 (2002).
- <sup>14</sup>D. W. Brenner, Phys. Rev. B **42**, 9458 (1990); J. Tersoff, Phys. Rev. Lett. **61**, 2879 (1988).
- <sup>15</sup>D. H. Robertson, D. W. Brenner, and J. W. Mintmire, Phys. Rev. B **45**, 12 592 (1992).
- <sup>16</sup>See, for example, M. B. Nardelli, B. I. Yakobson, and J. Bernholc, Phys. Rev. Lett. **81**, 4656 (1998); B. I. Yakobson, C. J. Brabec, and J. Bernholc, *ibid.* **76**, 2511 (1996); Yueyuan Xia, Yuchen Ma, Yuelin Xiang, Yuguang Mu, Chunyu Tan, and Liangmo Mei, Phys. Rev. B **61**, 11 088 (2000).
- <sup>17</sup>N. G. Chopra, L. X. Benedict, V. H. Crespi, M. L. Cohen, S. G. Louie, and A. Zettl, Nature (London) **377**, 135 (1995).
- <sup>18</sup>L. F. Sun, S. S. Xie, W. Liu, W. Y. Zhou, Z. Q. Liu, D. S. Tang, G. Wang, and L. X. Qian, Nature (London) **403**, 384 (2000).
- <sup>19</sup>A. Incze, A. Pasturel, and P. Peyla, Phys. Rev. B **66**, 172101 (2002).
- <sup>20</sup>P. C. Sanfelix, S. Holloway, K. W. Kolasinski, and G. R. Darling, Surf. Sci. **532**, 166 (2003).
- <sup>21</sup>S. P. Chan, W. L. Yim, X. G. Gong, and Z. F. Liu, Phys. Rev. B **68**, 075404 (2003).
- <sup>22</sup>L. D. Landau and E. M. Lifshitz, *Elasticity Theory* (Pergamon, Oxford, 1996).
- <sup>23</sup>S. Timoshenko and J. Gore, *Theory of Elastic Stability* (McGraw-Hill, New York, 1988).
- <sup>24</sup>A. Li, Feng Liu, and M. G. Lagally, Phys. Rev. Lett. **85**, 1922 (2000).
- <sup>25</sup>T. Hertel, R. E. Walkup, and P. Avouris, Phys. Rev. B **58**, 13 870 (1998).